Biocompatibility of Asiga Dental Resins Using a Low-Cost Printer for Biohybrid Actuator Applications

Ashlee S. Liao[1(✉)], Kevin Dai[1], Bhavya Chopra[1], Saul Schaffer[1], Rebekah Adams[1], Ji Min Seok[1], Alaeddin Burak Irez[1,2,3], Yongjie Jessica Zhang[1,2], and Victoria A. Webster-Wood[1,2,4]

[1] Department of Mechanical Engineering, Carnegie Mellon University, Pittsburgh, PA 15217, USA
{ashleel,kdai,bchopra,sschaffe,raadams, jseok2,airez,jessicaz,vwebster}@andrew.cmu.edu

[2] Department of Biomedical Engineering, Carnegie Mellon University, Pittsburgh, PA 15217, USA

[3] Department of Mechanical Engineering, Faculty of Mechanical Engineering, Istanbul Technical University (ITU), Istanbul, Turkey

[4] McGowan Institute for Regenerative Medicine, University of Pittsburgh 4200 Fifth Ave, Pittsburgh, PA 15260, USA
http://engineering.cmu.edu/borg, https://www.meche.engineering.cmu.edu/faculty/zhang-computational-bio-modeling-lab.html

Abstract. Biohybrid actuators and robots require the integration of biological materials with synthetic materials. Synthetic materials provide structural support and attachment points for biological materials. One technique for fabricating these synthetic support structures is 3D printing. Although some 3D-printable resins have been designed to be biocompatible, the process for assessing biocompatibility is not reported consistently. Furthermore, the ISO 10993-1 standard emphasizes that biocompatibility must be evaluated based on specific use cases. Therefore, for biohybrid actuator applications, two commercial Asiga dental resins, DentaGUIDE and DentaGUM, were printed using a low-cost, LCD resin printer (Phrozen Sonic Mini 8K) and analyzed for their biocompatibility with C2C12, a muscle cell line commonly used in biohybrid actuators. C2C12 cells were cultured in direct contact with resin samples for 72 h, and their viability was examined using ethidium homodimer-1 and calcein acetoxymethyl ester (calcein AM), fluorescent dyes that mark dead and live cells, respectively. The ratio of calcein AM to ethidium homodimer 1 (CalAM:EthD-1) fluorescence was significantly larger for cultures exposed to the autoclaved ($4,941 \pm 1,122$) or ethanol-sterilized ($3,783 \pm 683$) DentaGUIDE samples as compared to the ratio for cultures exposed to polydimethylsiloxane (PDMS) (autoclaved: $1,940 \pm 989$, ethanol-sterilized: 345 ± 446). The CalAM:EthD-1 ratio measured in cultures exposed to DentaGUM (autoclaved: 43.67 ± 9.38, ethanol-sterilized: 101.7 ± 86.0) was significantly lower than the ratio found for autoclaved

N. S. Szczecinski et al. (Eds.): Living Machines 2024, LNAI 14930, pp. 399–412, 2025.
https://doi.org/10.1007/978-3-031-72597-5_27

PDMS. This analysis suggested that DentaGUIDE has little to no impact on the health of C2C12, but DentaGUM negatively impacted the culture. Therefore, DentaGUIDE could be a suitable rigid material choice for biohybrid actuators.

Keywords: Resin 3D Printing · Biocompatibility · Biohybrid

1 Introduction

Naturally occurring biological actuators, such as muscle tissue, demonstrate several qualities that are difficult to achieve in artificial robotic actuation [34]. Biological tissues are naturally compliant, biodegradable, capable of self-healing, and are found in nature at a wide range of size scales [30]. To integrate these inherent biological qualities with robotic systems, biohybrid actuators combine living and synthetic materials. Synthetic materials, such as polydimethylsiloxane (PDMS), can be used to support muscle cells and tissues [11]. However, current biohybrid actuators do not have comparable performance with that of natural muscle [30].

One potential method to improve the performance of biohybrid muscle actuators is to incorporate synthetic substrates for supporting muscle maturation [30]. For example, scaffolds with micropatterns can help promote myoblast differentiation and myotube assembly in 2D cultures [14,29]. In addition, larger cantilever beams have been used to form 3D muscle constructs to mimic densely packed tissues [6,27,32]. Scaffolds can also be fabricated using soft lithography [14,29,32], which utilizes planar silicon wafers etched with patterns. However, using these planar silicon wafers makes fabricating more complex 3D structures beyond pillars or planar patterns challenging. Furthermore, etching patterns into the silicon wafer requires photolithographic techniques that need specialized equipment and clean rooms, which can reduce the accessibility of such methods.

For more complex 3D scaffold designs, resin-based 3D printing could be a viable, easily accessible method while maintaining high resolution (e.g., Formlabs Form 3+ series [8], Asiga MAX X27 [3], Phrozen Sonic Mini 8K [26]). Within the resin-printing industry, several resins, such as select Asiga [2] and Formlabs [9] dental resins, have been developed to be biocompatible. For engineered muscle strips, both custom [27] and commercial [6] resins have been explored. However, these specialized resins are commonly optimized for specific printers, such as the Asiga MAX series [3] or Formlabs Form 3B+ [7]. The starting cost of these commercial printers starts at several thousand USD (Table 1), which may limit the accessibility to such equipment. In contrast, the cost of consumer resin printers, such as the Phrozen Sonic Mini series, is commonly a few hundred USD (Table 1). However, printers from different manufacturers may use different technologies (Table 1, "Printer Type"). Thus, for fabricating using low-cost printers, the printing conditions must be optimized for each resin and printer. Additionally, due to differences in fabrication procedures, the biocompatibility of samples printed on an alternate printer must be reevaluated.

Table 1. Printing resolutions and costs of current resin printers on the market. For the printer types, the following acronyms are used: LCD - Liquid-Crystal Display; SLA - Stereolithography; DLP - Digital Light Processing. Note: for the Formlabs Form 3+, the resolution was determined as the laser spot size (the reported XY resolution).

Manufacturer	Printer	Printer Type	Resolution (μm)	Cost (USD, April 2024)	Ref.
Phrozen	Sonic Mini 8K	LCD	22	$485	[26]
Formlabs	Form 3B+	SLA	85(25)	$4,429	[7,8]
Asiga	MAX X27	DLP	27	$9,990	[3,5]

Not only would changing the printer necessitate a reevaluation of biocompatibility, the characterization of biocompatible resins has differed among different laboratories [12] and is often not clearly reported by manufacturers, even with the use of various certifications, such as CE marking or the International Organization for Standardization's (ISO) 10993 series of standards [13]. Furthermore, the ISO 10993-1:2018 standard specifies that biocompatibility tests should be designed and used for specific material usages [16]. As such, commercial resins that have been reported for biocompatibility to be used in medical devices should be reassessed for their applicability to biohybrid systems.

This work investigated two commercially available resins for their applicability to biohybrid actuators: Asiga [2] DentaGUIDE and DentaGUM. Asiga DentaGuide, which is used for fabricating surgical guides, is advertised to be biocompatible (CE Class I) and autoclavable [2], which are necessary qualities for usage with biological materials in biohybrid devices. DentaGUM is a flexible resin designed to mimic the gingiva, which might provide a suitable environmental stiffness for myocyte differentiation. There were no sterilization recommendations by the manufacturer for DentaGUM. Both materials' biocompatibility was evaluated in direct contact with C2C12, a common immortalized mouse myoblast cell line used for biohybrid actuators. A direct contact assessment was selected to mimic culture conditions in a biohybrid actuator since biological and synthetic materials must be well integrated.

2 Methods

DentaGUIDE and DentaGUM (Asiga, Ann Arbor, MI, USA) were evaluated for their biocompatibility for use in biohybrid devices. Samples of each resin were printed on a Phrozen Sonic Mini 8K resin printer (Phrozen Tech Co., LTD., Hsinchu, Taiwan), which is a low-cost (<$1,000) LCD resin 3D printer (Table 1). These samples were designed to be cylinders with a 2 mm diameter, which produces a flat face that would occupy at least 10% of the surface area of a well in a 96-well plate, as recommended by ISO 10993:5:2009 [15]. These samples were sterilized by a 70% ethanol soak or by autoclaving, two common techniques used for sterilization before being introduced into an ongoing C2C12 culture to assess biocompatibility. Six samples were used for each resin per sterilization technique.

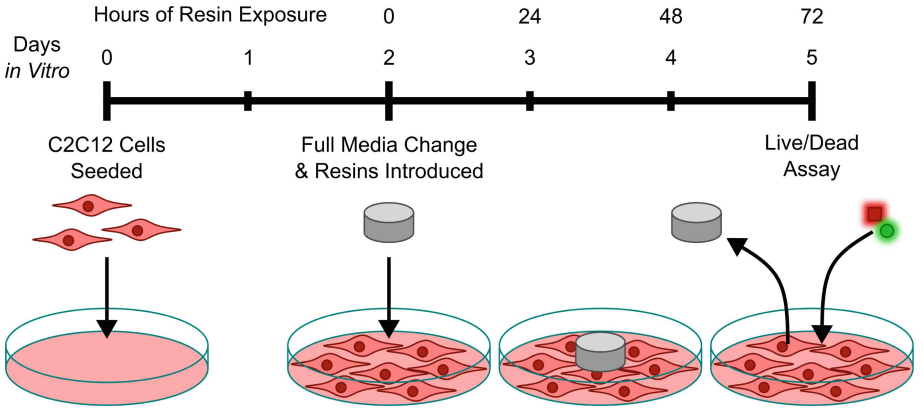

Fig. 1. Cells were seeded and cultured for 2 days before the introduction of a resin sample. After 72 h of incubation with the resin sample, a live/dead assay was used to evaluate biocompatibility.

2.1 Fabrication of Samples

The resins were printed on a Phrozen Sonic Mini 8K resin printer (Phrozen Tech Co., LTD., Hsinchu, Taiwan). Immediately after printing, they were washed in isopropanol for 5 min in an ultrasonic bath. This wash was repeated once in a second container of isopropanol. Following these washes, the samples were placed in a Phrozen Curing Station (Phrozen Tech Co., LTD., Hsinchu, Taiwan) with a 30-minute fan period and subsequent 15-minute cure period. Afterward, the samples were flipped over for a second 15-minute cure period.

For the negative controls, PDMS (SYLGARD 184; Dow Corning, Midland, MI, USA) samples were used. The samples were fabricated using a 10:1 base-to-curing-agent (w/w) ratio. A 2 mm biopsy punch was used to cut the PDMS samples.

2.2 Sample Sterilization

After the sample preparation, the samples were sterilized using one of two methods: soaking in 70% ethanol or autoclaving. For the ethanol soak, the samples were submerged in 70% ethanol for 1 h, after which they were washed three times in sterile, phosphate-buffered saline (PBS) (10-010-049; Gibco ThermoFisher, Waltham, MA, USA). They were then dried in ambient conditions in a biosafety cabinet (1300 Series A2, Model 1377; ThermoFisher, Waltham, MA, USA) with a single 1-hour ultraviolet light cycle. For the autoclave (ADV-PRO; Consolidated Sterilizer Systems, Billerica, MA, USA) procedure, the samples were subjected to a gravity cycle for 45 min at 121 °C, followed by a drying period of 15 min.

2.3 Cell Culture

Cryopreserved C2C12 cells were thawed and plated into a black-walled 96-well plate (655087; Greiner Bio-One, Kremsmünster, Austria) at their 9th passage at a density of 2,100 cells/well (≈6,200 cells/cm^2). For the entire period, the cells were cultured in a growth medium composed of 1% L-glutamine (200 mM, 25030081; Gibco ThermoFisher, Waltham, MA, USA), 1% penicillin-streptomycin (10,000 U/mL, 15140122; Gibco ThermoFisher, Waltham, MA, USA)), and 10% fetal bovine serum (A5256801; Gibco ThermoFisher, Waltham, MA, USA) in high glucose Dulbecco's Minimum Essential Medium (11965126; Gibco ThermoFisher, Waltham, MA, USA). For the duration of the culture, the cells were in an incubator that maintained 37 °C and 5% CO_2 conditions. The cells were cultured for two days and exhibited an average of 20–30% confluency before a complete medium change and the addition of resin samples (Fig. 1). After 72 h of incubation with the resin samples, a viability/cytotoxicity assay was conducted (Sect. 2.4, Fig. 1).

Six replicates were performed per resin and sterilization method. In addition, six replicates were performed for the PDMS negative control samples per sterilization method. Lastly, 12 wells were not exposed to any resin samples. Of these wells, 6 were blanks in which they were expected to contain a healthy, living population of cells. The remaining six wells were the positive, dead-cell controls and exposed to cold 70% ethanol for 15 min just prior to the viability/cytotoxicity assay.

2.4 Cytotoxicity Analysis

To test for biocompatibility, a viability/cytotoxicity assay (L3224; Invitrogen ThermoFisher, Waltham, MA, USA) was conducted using ethidium homodimer-1 to stain dead cells and calcein acetoxymethyl ester (calcein AM) to stain live cells as per the manufacturer's protocol [25]. Before staining, the resin and PDMS samples were carefully removed from the wells using sterile forceps. Afterward, the medium was removed from all wells. Then, the wells were washed three times with PBS. After removing PBS from the final wash, 100 μL of PBS was added to each well.

For staining the cells, 100 μL of 2 μM calcein AM and 4 μM ethidium homodimer-1 were added to each well that originally contained either a resin or PDMS sample, resulting in a final concentration of 1 μM calcein AM and 2 μM ethidium homodimer-1. As controls, for the wells that did not have any sample exposure (the live-cell blanks and dead-cell positive controls), only 100 μL of 2 μM calcein AM was added to half of the wells, resulting in a final concentration of 1 μM, as per manufacturer's protocol [25]. For the remaining half, 100 μL of 4 μM ethidium homodimer-1 was added, resulting in a final concentration of 2 μM. These wells were separately stained to ensure the expected fluorescence from each dye. All wells were incubated at room temperature for 30–60 min before their fluorescence intensities were measured using a plate reader (Synergy H1; Agilent BioTek, Santa Clara, CA, USA). Since the fluorescence intensities

are linearly proportional to the number of cells [25], the relative fluorescence units measured by the plate reader were used instead of cell count.

The cultures were imaged using brightfield and epifluorescence in an inverted microscope (Revolution; Echo Bico, San Diego, CA, USA) with a 10X objective lens. The brightfield camera used a 5 MP CMOS color camera, whereas the fluorescence camera used a 5 MP CMOS mono camera. FITC and Texas Red LED light cubes were used to visualize the calcein-AM and ethidium homodimer-1, respectively.

2.5 Statistics

The fluorescence intensity data collected from the plate reader was statistically analyzed using Minitab 2023 (v 21.4.2; Minitab, LLC, State College, PA, USA). The data was first assessed for normality using the Anderson-Darling test [21] and for equal variances using the Bartlett test [22]. Based on the results from this initial analysis, a balanced analysis of variance (ANOVA) [20] with a significance level of 0.05 and a post-hoc pairwise Bonferroni multiple comparison test between groups [23] was used for analyzing the data.

3 Results and Discussion

Based on the brightfield microscopy images, cultures exposed to DentaGUIDE and PDMS exhibited similar morphology as the live cell (blank) controls with >90% confluency (Fig. 2A–H). The C2C12 cell layer also grew close to the DentaGUIDE samples, but qualitatively, there appeared to be less growth near the autoclaved DentaGUIDE samples (Fig. 2E, G). Additionally, cultures exposed to DentaGUM exhibited a much lower density (<10% confluency) with a rounded cell morphology, with very few cells found near the DentaGUM samples (Fig. 2I–L).

After the PBS washing and application of the calcein AM and ethidium homodimer-1 stains to quantify the viability, fewer cells were found remaining in the wells exposed to DentaGUM (Fig. 3G,J) than before these steps (Fig. 2I–L). Before the wash and dye application, several cells exhibited a rounded morphology, which indicates that these cells were likely dying and beginning to detach from the culture surface. As such, a number of these dead or dying cells could be aspirated during the PBS wash steps prior to the dye loading. Although this reduction is most clearly observed for cultures exhibiting mostly rounded cell morphology, such as the DentaGUM exposed cultures, this could reduce the ethidium homodimer-1 fluorescence intensities reported by the plate reader for all of the cultures.

Unlike the rounded cells, the live, healthy cells were expected to remain attached to the culture surface during the PBS wash steps. However, the empty regions and highly dense regions observed in the culture for the blank (live cells with no resin or PDMS exposure) control indicated that the cells began

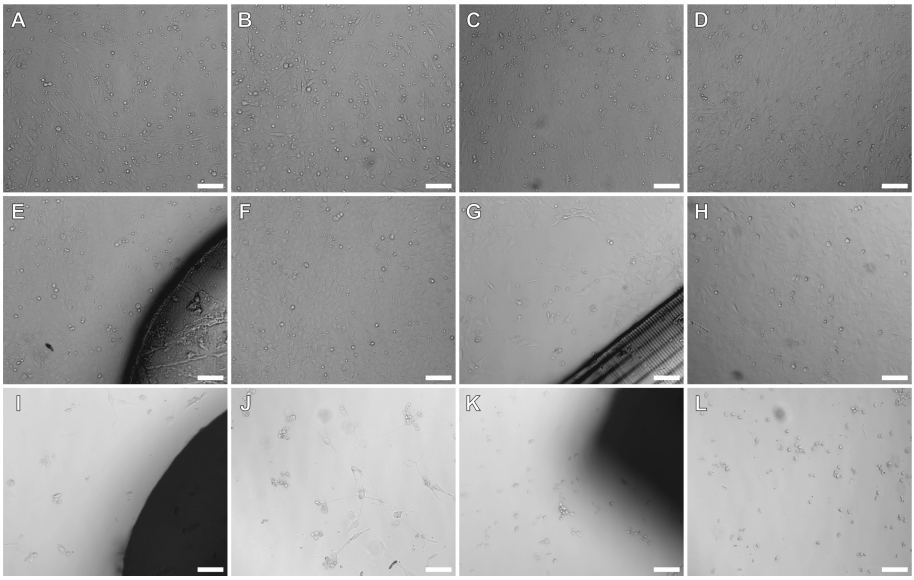

Fig. 2. Brightfield images of C2C12 cultures prior to loading calcein AM and ethidium homodimer-1. The top row illustrates the controls: (**A**) blank (live cell), (**B**) positive control (live cell at the time of imaging, just prior to exposure to ethanol for a dead cell control), (**C**) negative control (ethanol-sterilized PDMS), (**D**) negative control (autoclaved PDMS). The middle row illustrates cultures exposed to DentaGUIDE, that was (**E**-**F**) ethanol-sterilized and (**G**-**H**) autoclaved. The bottom row illustrates cultures exposed to DentaGUM, that was (**I**-**J**) ethanol-sterilized and (**K**-**L**) autoclaved. For (**E**), (**G**), (**I**), and (**K**), a portion of the resin sample was included in the image. Samples of PDMS could not be imaged with the cells since the PDMS tended to float in the culture medium. The scale bar in each subfigure represents 100 μm.

to detach from the surface after the PBS washes and dye application (Fig. 3A-B). This was also observed in the cultures exposed to PDMS and DentaGUIDE (Fig. 3E-F, H–I). This phenomenon was not as clearly observed in the cultures exposed to DentaGUM (Fig. 3G,J) since there was initially very little healthy cell attachment prior to the PBS wash steps and dye loading (Fig. 2I–K). However, the several DentaGUM cells tagged with the fluorescent dyes still exhibited a more rounded morphology, similar to the blank cultures.

Since PBS is non-toxic and isotonic, the wash steps were not expected to affect the cellular morphology or surface attachment. Therefore, the detachment of the cell layer could be attributed to the use of calcein AM, since calcein AM may be toxic to some cell lines [28]. Furthermore, since this was conducted as an endpoint assay and the fluorescence readings were done shortly after the dye application, the dye's impacts on long-term cell health would not affect the results in this study. Since the dyes are applied after the PBS washes, any affected live cells should remain in the wells and not affect the calcein AM fluo-

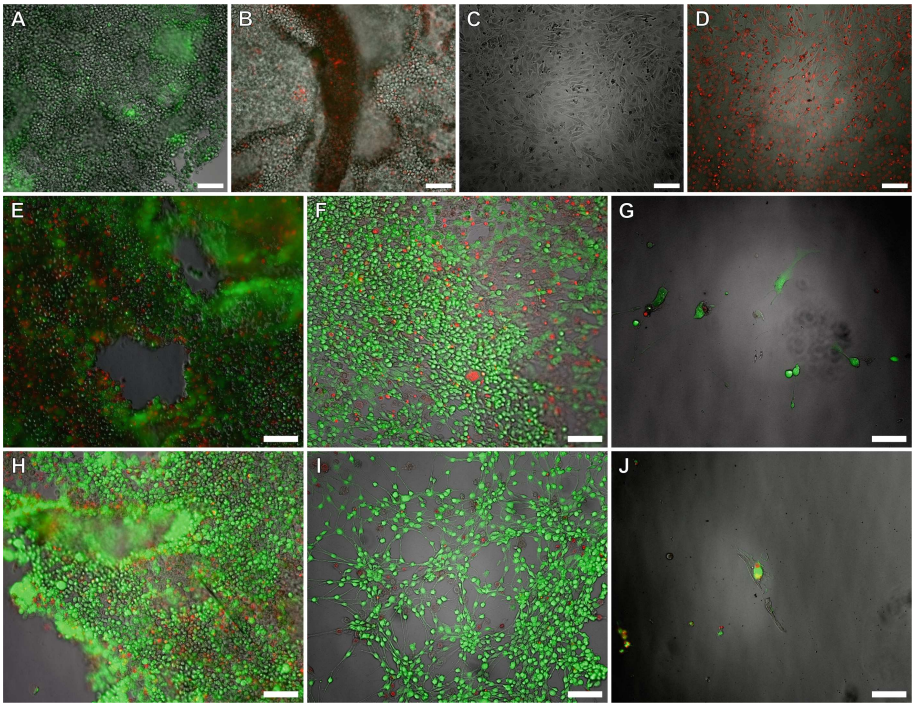

Fig. 3. Calcein AM (green) and ethidium homodimer-1 (red) fluorescent images overlaid images taken with transmitted light. Top row: blank (live cell) control (**A**-**B**) and the positive (dead cell) control (**C**-**D**). Cultures in (**A**) and (**C**) were loaded only with calcein AM. Middle row: cultures with ethanol-sterilized samples: (**E**) PDMS (negative control), (**F**) DentaGUIDE, (**G**) DentaGUM. Bottom row: cultures with autoclaved samples: (**H**) PDMS (negative control), (**I**) DentaGUIDE, (**J**) DentaGUM. Cultures in (**B**) and (**D**) were loaded only with ethidium homodimer-1. The remaining cultures were loaded with a combination of calcein AM and ethidium homodimer-1. The scale bar in each subfigure represents 100 μm. (Color figure online)

rescence intensities captured by the plate reader. Therefore, instead of comparing the individual fluorescence intensities of each dye, the ratio of the fluorescence intensities of calcein AM and ethidium homodimer-1 (CalAM:EthD-1) was used for the quantitative assessment of biocompatibility (Fig. 4).

The CalAM:EthD-1 responses for all groups exhibited normal distributions ($p > 0.05$), except ethanol-sterilized DentaGUM and PDMS ($p \leq 0.05$). Since a majority of the groups were normal, the Bartlett method was selected for the test for equal variances, in which the groups were determined to not have equal variances ($p = 0.000$). Based on these results, a balanced ANOVA was determined to be the appropriate statistical analysis since it is not sensitive to unequal variances if there are only fixed factors and equal sample sizes [22].

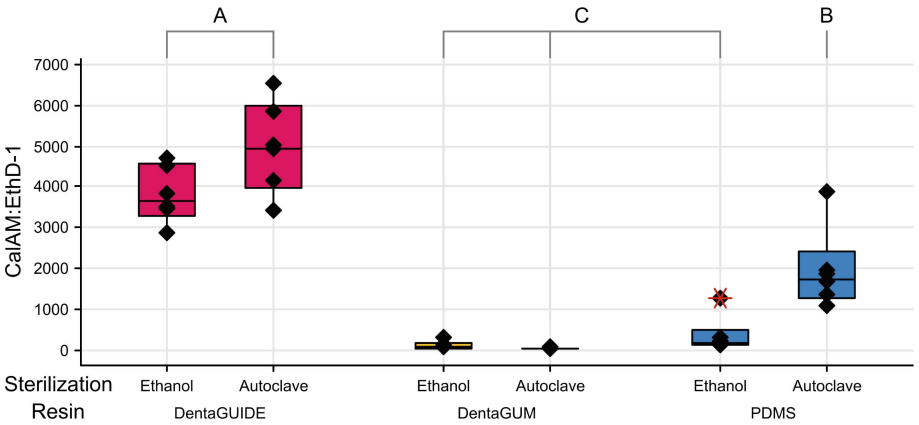

Fig. 4. Box plots of the CalAM:EthD-1 responses for each sterilization and resin condition. The first and third quartiles are represented by the bottom and top lines of each box, respectively. The minimum and maximum, excluding outliers, are represented by the whiskers extending from the interquartile range boxes. The median is represented by the middle line of each box. The black diamonds (♦) are the individual data points. Outliers are marked by a red asterisk (∗). The grouping results from the Bonferroni pairwise comparisons (Table 3 are also denoted in the boxplots in which conditions that do not share a letter are significantly different. (Color figure online)

The balanced ANOVA indicated significant associations between CalAM:EthD-1 and the resin type, sterilization mode, and the interaction effect between the resin type and sterilization mode ($p < 0.05$, Table 2). This is indicative that the means are not equal and that the effects of the resin and sterilization mode should be considered together.

Since the ANOVA indicated significant differences based on the sterilization method and the resin type, a post-hoc Bonferroni pairwise comparison was conducted to identify which groups were significantly different (Table 3, Fig. 4). The autoclaved and ethanol-sterilized DentaGUIDE samples demonstrated sig-

Table 2. Balanced ANOVA of CalAM:EthD-1 results. The Source lists the factors (Sterilization and Resin) and interactions between the factors (Sterilization*Resin) considered. DF: degrees of freedom per source; SS: adjusted sum of squares. MS: adjusted mean squares; F: ANOVA test statistic; p is the probability value.

Source	DF	SS	MS	F	p
Sterilization	1	7,266,940	7,266,940	14.99	0.001
Resin	2	119,621,488	59,810,744	123.39	0.000
Sterilization*Resin	2	4,403,350	2,201,675	4.54	0.019
Error	30	14,542,365	484,745		
Total	35	145,834,143			

nificantly larger CalAM:EthD-1 means than the means of the PDMS samples, which suggests that DentaGUIDE has little impact on cell viability. In addition, the DentaGUM CalAM:EthD-1 means were significantly lower than the means from the autoclaved PDMS samples, which suggests that DentaGUM negatively impacts the health of the culture. Both the DentaGUIDE and DentaGUM conclusions are in alignment with the morphology observed prior to the introduction of the dyes (Fig. 2).

In addition to considering different resin types for biohybrid devices, sterilization techniques are also important in tissue engineering [4]. For example, PDMS slightly swells after ethanol immersion [18], but the mechanical properties are altered after steam autoclaving [19,24]. Therefore, an appropriate sterilization technique must be selected based on desired bioactuator functions. In this study, when investigating the impacts on sterilization techniques in conjunction with the resin type, there was not a significant difference between the responses to ethanol-sterilized DentaGUIDE and autoclaved DentaGUIDE (Table 3, Fig. 4). This indicates either technique is acceptable for sterilizing DentaGUIDE, but additional studies should be conducted to investigate any impacts of sterilization on the mechanical properties of DentaGUIDE. Although the cellular responses to sterilization techniques on DentaGUIDE were not significantly different, there was an unexpected, significant difference between the responses to ethanol-sterilized PDMS and autoclaved PDMS (Table 3, Fig. 4) since both techniques are commonly used for sterilizing PDMS [19,24]. This might suggest that the impacts of ethanol exposure on PDMS, such as swelling [18], could impact the C2C12 culture, but additional study is needed to explore this.

Furthermore, since PDMS is known to be a biocompatible, inert elastomer [24], the lower CalAM:EthD-1 means, as compared to those of DentaGUIDE, were also unexpected (Table 3, Fig. 4). The lower PDMS means could potentially be attributed to the resin removal process prior to the washing and dye loading procedures. PDMS samples tended to float in the culture medium, which caused their removal via forceps to be more challenging than the DentaGUIDE samples that rested at the bottom of the wells. In turn, this could have caused the PDMS samples to move more during the removal process and act as a cell scraper. Any cells detached from the culture surface during the resin removal process will likely be aspirated during the wash steps before the loading of the dye. Therefore, the removal of these cells could reduce the CalAM:EthD-1 response of PDMS. In future work, elution studies, an indirect biocompatibility test using sample extracts, can be performed to verify this theory (ISO 10993-5 [15] and ISO 10993-12 [17]). However, using only sample extracts will not adequately mimic biohybrid use cases since it would only test for the impacts of potential leachants. Since the biological materials will be physically integrated with the synthetic materials, direct contact testing more closely represents the environment living cells will experience in a biohybrid system.

In addition to exploring elution studies to complement direct testing, the use of additional cell viability assessments could further the understanding of the impacts of the resin on C2C12. Calcein AM specifically tags for intracel-

Table 3. Post-hoc Bonferroni pairwise comparison between factors for each type of source: sterilization, resin, and combination of the sterilization and resin. For each source, means with a different letter are significantly different (i.e., factors that are assigned to "A" are significantly different from factors assigned to "B" within the same source).

Factor		N	Mean ± Standard Deviation	Grouping		
Sterilization						
Autoclave		18	2,308 ± 2,228		A	
Ethanol		18	1,410 ± 1,786			B
Resin						
DentaGUIDE		12	4,362 ± 1,072	A		
PDMS		12	1,143 ± 1,108		B	
DentaGUM		12	72.7 ± 65.8			C
Sterilization	**Resin**					
Autoclave	DentaGUIDE	6	4,941 ± 1,122	A		
Ethanol	DentaGUIDE	6	3,783 ± 683	A		
Autoclave	PDMS	6	1,940 ± 989		B	
Ethanol	PDMS	6	345 ± 446			C
Ethanol	DentaGUM	6	101.7 ± 86.0			C
Autoclave	DentaGUM	6	43.67 ± 9.38			C

lular esterase activity, which is typically present in living cells, while ethidium homodimer-1 binds to nucleic acids, but can only pass through damaged plasma membranes that are typical of dead cells [25]. In addition, there was a noticeable impact on the cellular morphology with the use of calcein AM and ethidium homodimer. Another cell viability assay, such as measuring the extracellular concentration of lactate dehydrogenase (LDH) which is only released when with the loss of plasma membrane integrity [1], could be explored. Furthermore, calcein AM/homodimer-1 assays and LDH assays can be suitable for assessing cell viability in 3D tissues [10]. However, the use of LDH, calcein AM, and ethidium homodimer will not inform if the resins have impacts on other aspects of cellular activity. To investigate this, other cell viability assays, such as tetrazolium-based assays (*e.g.* 3-(4,5-dimethylthiazol-2-yl)-2,5-diphenyltetrazolium bromide (MTT) tetrazolium reduction assays) for metabolism [31] or 5-ethynyl-2'-deoxyuridine (EdU) for proliferation [33], could complement the calcein AM and ethidium homodimer-1 results in this study. In addition to studying the effects on metabolism and proliferation, this study can be extended to investigate the impacts on C2C12 differentiation, which is crucial for the maturation of contractile myotubes necessary for functional biohybrid actuators [30]. The use of these additional assays as well as the same calcein AM/ethidium homodimer-1 viability assay in a 3D culture can further validate DentaGUIDE's applicability to future biohybrid actuators.

4 Conclusion

In biohybrid actuators, synthetic material components are used to support living materials, such as muscle. For fabricating these supportive, synthetic structures, 3D printing is one avenue that can be used for producing complex structures. However, the biocompatibility assessment of resins is not clearly reported by manufacturers. Furthermore, the assessment cannot be generalized and must be designed for specific use cases. Therefore, for the use in biohybrid actuator fabrication, the biocompatibility of two commercial resins, Asiga DentaGUIDE and DentaGUM, was evaluated. Cultures of C2C12, a common muscle cell line used in biohybrid actuators, were exposed to DentaGUIDE and DentaGUM samples for 72 h. Based on the observed morphology and a viability/cytotoxicity assay, DentaGUIDE was found to have minimal impact on the culture health, whereas DentaGUM negatively impacted the culture. Therefore, DentaGUIDE is likely suitable as a rigid supporting structure for biohybrid actuators, but more soft, elastomeric materials need to be explored.

Acknowledgments. This material is based upon work supported by the National Science Foundation (NSF). ASL and SS were supported by the Graduate Research Fellowship Program under Grant No. DGE1745016. This work was also supported by the NSF Faculty Early Career Development Program under Grant No. ECCS-2044785. Any opinions, findings, and conclusions or recommendations expressed in this material are those of the author(s) and do not necessarily reflect the views of the NSF. This research was also sponsored by the Army Research Office and was accomplished under Cooperative Agreement Number W911NF-23-2-0138. The views and conclusions contained in this document are those of the authors and should not be interpreted as representing the official policies, either expressed or implied, of the Army Research Office or the U.S. Government. The U.S. Government is authorized to reproduce and distribute reprints for Government purposes notwithstanding any copyright notation herein. KD was also supported by the Innovation Commercialization Fellowship from Carnegie Mellon University (CMU). ABI gratefully acknowledges financial support for this publication by the Fulbright Post Doctoral Program, which is sponsored by the U.S. Department of State and Turkish Fulbright Commission. For ASL, funding to attend this conference was partially provided by the CMU Graduate Student Association (GSA)/Provost Conference Funding.

References

1. Allen, M., Millett, P., Dawes, E., Rushton, N.: Lactate dehydrogenase activity as a rapid and sensitive test for the quantification of cell numbers in vitro. Clin. Mater. **16**(4), 189–194 (1994). https://doi.org/10.1016/0267-6605(94)90116-3
2. Asiga: Materials Dental - Asiga (2024). https://www.asiga.com/materials-dental/
3. Asiga: Max X - Asiga (2024). https://www.asiga.com/max-x/
4. Dai, Z., Ronholm, J., Tian, Y., Sethi, B., Cao, X.: Sterilization techniques for biodegradable scaffolds in tissue engineering applications. J. Tissue Eng. **7**, 204173141664881 (2016). https://doi.org/10.1177/2041731416648810
5. DELRAY Systems: Asiga MAX X (2019). https://www.3d-printer.com/products/asiga-max-x/163943000017772029

6. Finkel, S., et al.: FRESH^{TM} 3D bioprinted cardiac tissue, a bioengineered platform for in vitro pharmacology. APL Bioeng. **7**(4), 046113 (2023). https://doi.org/10.1063/5.0163363
7. Formlabs: Form 3B+ (2024). https://formlabs.com/3d-printers/form-3b/
8. Formlabs: Formlabs Stereolithography 3D Printers Tech Specs (2024). https://formlabs.com/3d-printers/form-3/tech-specs/
9. Formlabs Dental: Materials (2024). https://dental.formlabs.com/store/materials/?Biocompatible=5457
10. Gantenbein-Ritter, B., Potier, E., Zeiter, S., Van Der Werf, M., Sprecher, C.M., Ito, K.: Accuracy of three techniques to determine cell viability in 3D tissues or scaffolds. Tissue Eng. Part C Methods **14**(4), 353–358 (2008). https://doi.org/10.1089/ten.tec.2008.0313
11. Gao, L., et al.: Recent progress in engineering functional biohybrid robots actuated by living cells. Acta Biomater. **121**, 29–40 (2021). https://doi.org/10.1016/j.actbio.2020.12.002
12. Gruber, S., Nickel, A.: Toxic or not toxic? The specifications of the standard ISO 10993–5 are not explicit enough to yield comparable results in the cytotoxicity assessment of an identical medical device. Front. Med. Technol. **5**, 1195529 (2023). https://doi.org/10.3389/fmedt.2023.1195529
13. Guttridge, C., Shannon, A., O'Sullivan, A., O'Sullivan, K.J., O'Sullivan, L.W.: Biocompatible 3D printing resins for medical applications: A review of marketed intended use, biocompatibility certification, and post-processing guidance. Annals 3D Printed Med. **5**, 100044 (2022). https://doi.org/10.1016/j.stlm.2021.100044
14. Huang, N.F., et al.: Myotube assembly on nanofibrous and micropatterned polymers. Nano Lett. **6**(3), 537–542 (2006). https://doi.org/10.1021/nl060060o
15. International Organization for Standardization: ISO 10993-5:2009: Biological evaluation of medical devices Part 5: Tests for in vitro cytotoxicity (2009). https://www.iso.org/standard/36406.html
16. International Organization for Standardization: ISO 10993-1:2018: Biological evaluation of medical devices Part 1: Evaluation and testing within a risk management process (2018). https://www.iso.org/standard/68936.html
17. International Organization for Standardization: ISO 10993-12:2021: Biological evaluation of medical devices Part 12: Sample preparation and reference materials (2021). https://www.iso.org/standard/75769.html
18. Lee, J.N., Park, C., Whitesides, G.M.: Solvent compatibility of poly(dimethylsiloxane)-based microfluidic devices. Anal. Chem. **75**(23), 6544–6554 (2003). https://doi.org/10.1021/ac0346712
19. Mata, A., Fleischman, A.J., Roy, S.: Characterization of polydimethylsiloxane (PDMS) properties for biomedical micro/nanosystems. Biomed. Microdev. **7**(4), 281–293 (2005). https://doi.org/10.1007/s10544-005-6070-2
20. Minitab Support: Methods and formulas for Balanced ANOVA (2024). https://support.minitab.com/en-us/minitab/help-and-how-to/statistical-modeling/anova/how-to/balanced-anova/methods-and-formulas/methods-and-formulas/
21. Minitab Support: Methods and formulas for Graphical Summary (2024). https://support.minitab.com/en-us/minitab/help-and-how-to/statistics/basic-statistics/how-to/graphical-summary/methods-and-formulas/methods-and-formulas/
22. Minitab Support: Understanding test for equal variances (2024). https://support.minitab.com/en-us/minitab/help-and-how-to/statistical-modeling/anova/supporting-topics/basics/understanding-test-for-equal-variances/

23. Minitab Support: What is the Bonferroni method? (2024). https://support.minitab.com/en-us/minitab/help-and-how-to/statistical-modeling/anova/supporting-topics/multiple-comparisons/what-is-the-bonferroni-method/
24. Miranda, I., Souza, A., Sousa, P., Ribeiro, J., Castanheira, E.M.S., Lima, R., Minas, G.: Properties and applications of PDMS for biomedical engineering: a review. J. Funct. Biomater. **13**(1), 2 (2021). https://doi.org/10.3390/jfb13010002
25. Molecular Probes: LIVE/DEAD ® Viability/Cytotoxicity Kit *for mammalian cells* (2005). https://assets.thermofisher.com/TFS-Assets%2FLSG%2Fmanuals%2Fmp03224.pdf
26. Phrozen: Phrozen Sonic Mini 8K Resin 3D Printer. https://phrozen3d.com/products/sonic-mini-8k
27. Raman, R., Cvetkovic, C., Bashir, R.: A modular approach to the design, fabrication, and characterization of muscle-powered biological machines. Nat. Protoc. **12**(3), 519–533 (2017). https://doi.org/10.1038/nprot.2016.185
28. Ramirez, C.N., Antczak, C., Djaballah, H.: Cell viability assessment: toward content-rich platforms. Expert Opin. Drug Discov. **5**(3), 223–233 (2010). https://doi.org/10.1517/17460441003596685
29. Ricotti, L., Fujie, T., Vazão, H., Ciofani, G., Marotta, R., Brescia, R., Filippeschi, C., Corradini, I., Matteoli, M., Mattoli, V., Ferreira, L., Menciassi, A.: Boron nitride nanotube-mediated stimulation of cell co-culture on micro-engineered hydrogels. PLoS One **8**(8), e71707 (2013). https://doi.org/10.1371/journal.pone.0071707
30. Ricotti, L., et al.: Biohybrid actuators for robotics: a review of devices actuated by living cells. Science Robotics **2**(12), eaaq0495 (2017). https://doi.org/10.1126/scirobotics.aaq0495
31. Riss, T.L., et al.: Cell Viability Assays. In: Markossian, S., et al. (eds.) Assay Guidance Manual. Eli Lilly & Company and the National Center for Advancing Translational Sciences, Bethesda (MD) (2004). http://www.ncbi.nlm.nih.gov/books/NBK144065/
32. Sakar, M.S., et al.: Formation and optogenetic control of engineered 3D skeletal muscle bioactuators. Lab Chip **12**(23), 4976 (2012). https://doi.org/10.1039/c2lc40338b
33. Salic, A., Mitchison, T.J.: A chemical method for fast and sensitive detection of DNA synthesis in vivo. Proc. Natl. Acad. Sci. **105**(7), 2415–2420 (2008). https://doi.org/10.1073/pnas.0712168105
34. Webster-Wood, V.A., Akkus, O., Gurkan, U.A., Chiel, H.J., Quinn, R.D.: Organismal engineering: toward a robotic taxonomic key for devices using organic materials. Sci. Robot. **2**(12), eaap9281 (2017). https://doi.org/10.1126/scirobotics.aap9281